Delfim Pedrosa, Ricardo Gomes, Vitor Monteiro, Aparício Fernandes, João Monteiro, João L. Afonso

"Model Predictive Control of an On-Board Fast Battery Charger for Electric Mobility Applications"

CONTROLO Portuguese Conference on Automatic Control, Guimarães – Portugal, Sept. 2016.

https://link.springer.com/chapter/10.1007/978-3-319-43671-5_57

ISBN: 978-3-319-43670-8

DOI 10.1007/978-3-319-43671-5_57

Delfim Pedrosa, Ricardo Gomes, Vitor Monteiro, Aparício Fernandes, João Monteiro, João L. Afonso, "Model Predictive Control of a Fast Battery Charger for Electric Mobility Applications", CONTROLO Portuguese Conference on Automatic Control, Guimarães - Portugal, pp. 679-689, Sept. 2016. DOI: 10.1007/978-3-319-43671-5_57 ISBN: 978-3-319-43670-8 (Print) 978-3-319-43671-5 (Online)

Model Predictive Control of an On-Board Fast Battery Charger for Electric Mobility Applications

Delfim Pedrosa, Ricardo Gomes, Vitor Monteiro,
Aparício Fernandes, João Monteiro, João L. Afonso

Centro ALGORITMI, University of Minho, 4804-533, Guimarães, Portugal
{delfim.pedrosa,ricardo.gomes,vitor.monteiro,aparicio.fernandes,
joao.monteiro,joao.l.afonso}@algoritmi.uminho.pt

Abstract. Under the necessities of reducing emissions and air pollution, and also for increasing fuel economy, automotive companies have been developing electric and plug-in hybrid electric vehicles. Since these vehicles are parked when the batteries are being charged, it is possible to use the traction power converter as on-board charger, also allowing to reduce weight, volume and costs of components in the vehicle. In this context, this paper presents a model predictive control algorithm for an on-board fast battery charging that uses the traction power converter of an electric vehicle. Simulation results and system implementation are depicted, and finally, are presented some experimental results obtained with the proposed control system.

Keywords: Electric Vehicles, Fast Battery Charger, Model Predictive Control, G2V - Grid-to-Vehicle, V2G - Vehicle-to-Grid.

1 Introduction

Batteries are the most common source of energy for electric vehicles (EVs) [1]. Therefore, many charging systems have been developed in order to provide energy to the batteries of EVs, usually from the electrical power grid. EVs have typically two types of battery chargers: on-board and off-board (or standalone) charging systems [2].

On-board charging systems are installed inside the vehicle, and thus the cost, weight and space minimization are the main requirements considered [3]. Hence, this system is commonly implemented using low-power converters [3]. Commercially available on-board battery chargers have typical power density and weight of approximately 0.6 kW/kg and 6.2 kg, respectively [4]. Hence, the battery charging process has a typical duration of a few hours [5]. Unlike the off-board type, the on-board charging can be done, practically, in any location, as long as there is an electrical network outlet available [2], [6], for level 1 (slow) charging. Thus, this type of charging contributes to increase the acceptance of EVs and to reduce the cost of the infrastructure network for public charging [7].

A bidirectional power flow capability is also a relevant feature for a battery charger of an EV, since it provides some additional features. In addition to the normal battery charging process, known as grid-to-vehicle (G2V) operation mode, it also supports energy injection back to the electrical grid, known as vehicle-to-grid (V2G) operation mode, contributing to the development of the smart grids [6], [8]. Besides the G2V and V2G operation modes, a bidirectional battery charger can also be used to supply home loads during power outages, or to supply loads in places without connection to the power grid, known as vehicle-to-home (V2H) operation mode [8].

A battery charger can operate isolated (with galvanic isolation) or non-isolated from the electrical grid. Isolated chargers are preferred for safety reasons, but due to its impact on the vehicles' cost and weight they are usually avoided. Thus, most of the reported integrated chargers are non-isolated [2,3].

EVs have different power electronics converters, where the battery charger converter and the motor drive converter are the main converters. Due to the similarities between both, it is possible to join them together in a single power converter. It is important to note that this is only possible knowing that the motor drive and the battery charging operations are not performed simultaneously. This type of solution is identified in the literature as an integrated motor drive and battery charger, or simply as an integrated charger [9].

An integrated charger aims to reduce the size, number of components and the weight of the power converters in the EV. Ideally, the goal is to have an on-board battery charger without requiring any extra hardware in addition to the components of the motor drive system.

Fig. 1 presents a topology that concretizes both of these modes, motor drive and battery charger, in the same power converter. One interesting feature is associated with the compatibility with any electrical machines, with or without access to the neutral point. However, this solution requires a relay for disconnecting the electric machine during the battery charging process.

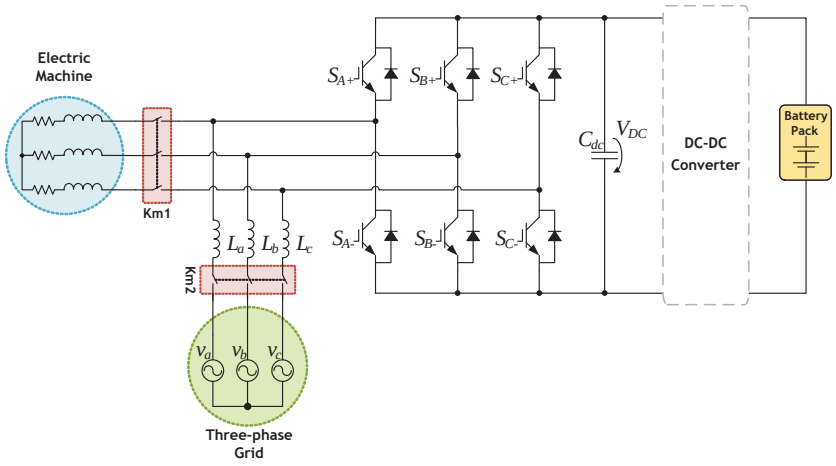

Fig. 1. Integrated power converter for EV motor drive or EV battery charger.

This topology allows the slow EV battery charging, but also is compatible with the fast EV battery charging through an AC three-phase power grid system. One of the main concerns regarding the battery charging operation is its influence on the power quality of the electrical grid. Therefore, the battery charging operation should be performed with unitary power factor and with consumption of almost sinusoidal currents, i.e., with low harmonic content [9,10].

The focus of this paper is the operation of an on-board fast battery charger that uses the traction power converter of an EV.

2 Predictive Control

Classic linear controllers with modulation techniques and nonlinear controllers based on hysteresis comparators are the most widely used in control algorithms. However, the developments achieved over the last years on digital electronics, including digital signal controllers (DSCs), offer more computational power, potentiating the development of new and more effective and complex control techniques, such as the model predictive control (MPC) [11].

In [12] is propose a type of finite control set model predictive control (FCS-MPC), mentioned as direct power control based on model predictive control (DPC-MPC), for controlling a boost AC-DC converter. The dynamical model of the three-phase boost AC-DC converter is shown in equation (1) and the derivative is described in equation (2), where, $v_s(t)$ is the power grid voltage, $v_R(t)$ is the voltage across the internal resistance of the inductor, $v_L(t)$ is the voltage across the inductor, $v_{in}(t)$ is the input voltage in converter, $R_s(t)$ is the internal resistance of the inductor, and $i_s(t)$ is the grid current.

$$v_s(t) = v_R(t) + v_L(t) + v_{in}(t) = R_s i_s(t) + L_s \frac{di_s(t)}{dt} + v_{in}(t) \tag{1}$$

$$\frac{di_s(t)}{dt} = \frac{1}{L_s}\left[v_s(t) - R_s i_s(t) - v_{in}(t)\right] \tag{2}$$

Using the forward Euler approximation, the derivative of the current is approximated to equation (3), and thus the input predicted current (i_s) is discretized for a sample period T_s, resulting in equation (4), where L_s is the inductance of the extra inductor.

$$\frac{di_s(t)}{dt} \cong \frac{i_s(k+1) - i_s(k)}{T_s} \tag{3}$$

$$i_s(k+1) = \left(1 - \frac{R_s T_s}{L_s}\right) i_s(k) + \frac{T_s}{L_s}\left[v_s(k) - v_{in}(k)\right] \tag{4}$$

To accommodate all the three-phase components of the system, the input currents and voltages are defined as space vectors, according to equation (5) and equation (6) respectively, where $\alpha = e^{j(2\pi/3)}$.

$$i_s = \frac{2}{3}\left(i_a + \alpha\, i_b + \alpha^2 i_c\right) \tag{5}$$

$$v_s = \frac{2}{3}\left(v_a + \alpha\, v_b + \alpha^2 v_c\right) \tag{6}$$

The voltage v_{in} is dependent on the switching state of the power electronics converter and the voltage of the DC-bus. In this case, [12] propose to define v_{in} as a space vector according to equation (7), and the value of S is defined according to equation (8), where S_a, S_b and S_c are the switching states of each leg of the converter.

$$v_{in} = S\, V_{DC} \tag{7}$$

$$S = \frac{2}{3}\left(S_a + \alpha\, S_b + \alpha^2 S_c\right) \tag{8}$$

Considering the space vector definitions used for the voltage and current values, the predicted values for the instantaneous real power (p) and imaginary power (q) are defined according to equation (9) and equation (10), respectively.

$$p(k+1) = v_{s\alpha}\, i_{s\alpha} + v_{s\beta}\, i_{s\beta} = \Re e\left\{v_s(k+1)\,\overline{i_s}(k+1)\right\} \tag{9}$$

$$q(k+1) = v_{s\beta}\, i_{s\alpha} - v_{s\alpha}\, i_{s\beta} = \Im m\left\{v_s(k+1)\,\overline{i_s}(k+1)\right\} \tag{10}$$

Using a high sampling frequency, it can be used the approximation defined by:

$$v_s(k+1) \approx v_s(k) \tag{11}$$

The MPC is based in the control of the instantaneous powers p and q and thus, in [12] is proposed a cost function g defined according to:

$$g = \left|q_{ref}(k) - q(k+1)\right| + \left|p_{ref}(k) - p(k+1)\right| \tag{12}$$

In real-time applications it is not possible to measure variables, predict their future values and apply the respective control action at the same instant. Thus, it is not correct to determine the predicted values considering that it is possible to apply the desired switching state at the same instant. Hence, to avoiding errors with the predictions, a delay in the predictive model has to be considered, resulting in a two-step-ahead prediction [12,13].

Since the selected voltage can only be applied at the next step (k+1), it is necessary to predict the current obtained as consequence of the select switching state, i.e., the

current at (k+2). This current is obtained by shifting equation (4) one step forward, resulting in:

$$i_s(k+2)=\left(1-\frac{R_sT_s}{L_s}\right)i_s(k+1)+\frac{T_s}{L_s}\left[v_s(k+1)-v_{in}(k+1)\right] \tag{13}$$

Thus, first time of $i_s(k+1)$ is calculated using equation (4), considering the current and voltage measured and the value of v_{in} obtained as consequence of the switching state selected in the previous sampling. Then, the obtained predicted current uses the equation (13).

In this paper, it is used the cost function:

$$g=\left|q_{ref}(k)-q(k+2)\right|+\left|p_{ref}(k)-p(k+2)\right|+\lambda C \tag{14}$$

The cost function includes a third component, with the purpose of overcoming the high frequency components around the commutation frequency. Before computing the cost function result, the control system checks if the switching state under analysis is equal to the last selected switching state. If it is equal, the value of C in equation (15) is set to 1, otherwise the value of C is set to 0. The parameter λ defines the weight of this component in the cost function.

Fig. 2 describes the MPC algorithm to perform the fast EV battery charger.

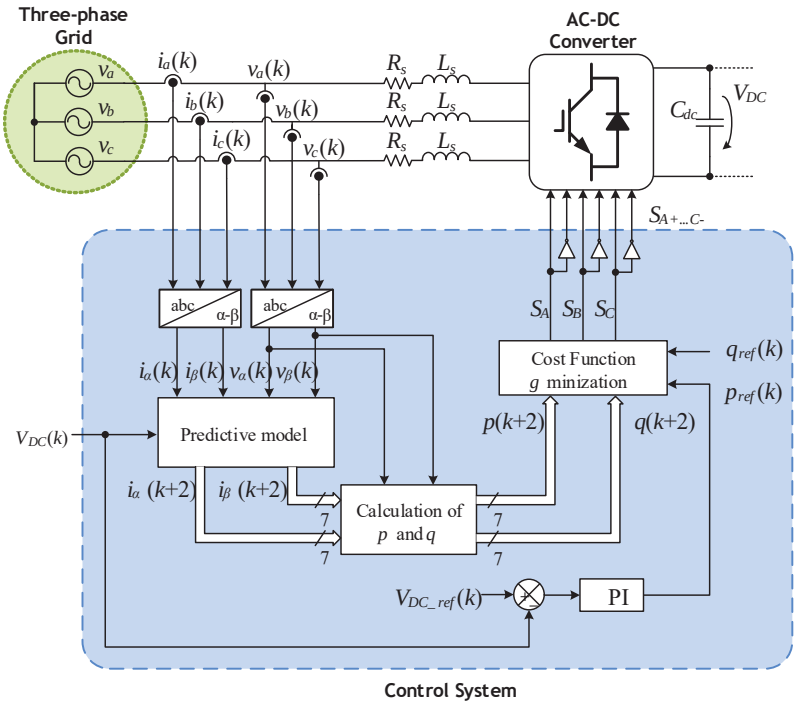

Fig. 2. Block diagram of the presented MPC algorithm.

3 Simulation Results

This section presents the main simulation results obtained to validate the model predictive control applied to a fast EV battery charger during the G2V operation mode. The simulations stage is a process of great importance, since it allows the anticipation of some problems that might occur in a real implementation. Hence, it contributes to the optimization of the time required for the development, as well as to reduce the financial resources required. The simulation results were obtained with the simulation software PSIM v9.0.

3.1 Grid-to-Vehicle Operation without Reactive Power Compensation

This section presents the simulation results considering an instantaneous real power reference (p_{ref}) of 15 kW and an instantaneous imaginary power reference (q_{ref}) of 0 kVAr. Fig. 3 (a) shows the obtained results of the instantaneous real power (p) and the instantaneous imaginary power (q), and the respective references (p_{ref}) and (q_{ref}). On the other hand, the obtained waveforms of the power grid voltages (v_a, v_b and v_c) and the grid currents (i_a, i_b and i_c) are shown in Fig. 3 (b). The measured RMS values, THD values and Power Factor of the grid currents are presented in Table 1.

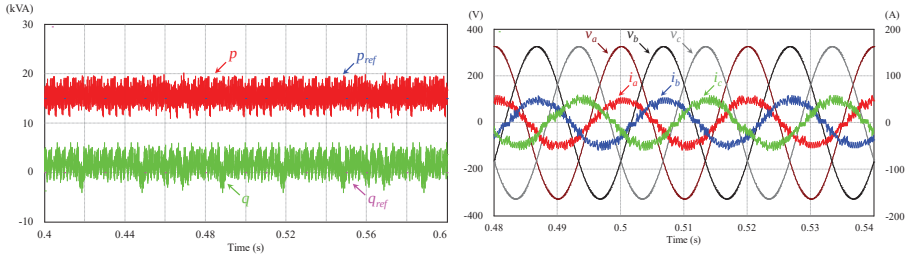

(a) (b)

Fig. 3. Simulation results of the fast EV battery charging process in steady-state: (a) Instantaneous p-q powers (p and q) and respective references (p_{ref} and q_{ref}); (b) Power grid voltages (v_a, v_b and v_c) and grid currents (i_a, i_b and i_c).

Table 1. Measured RMS values, THD values and Power Factor of the grid currents during the fast EV battery charging process.

	RMS	THD	Power Factor
i_a	34.97 A	15.42%	0.98
i_b	34.85 A	15.09%	0.98
i_c	34.92 A	16.20%	0.98

3.2 Grid-to-Vehicle Operation with Reactive Power Compensation

This section presents the main simulation results performed with a reference of the instantaneous imaginary power (q_{ref}) different from 0, i.e., the fast EV battery charger operates as a reactive power compensator.

The reference of the instantaneous real power (p_{ref}) is set to 15 kW. To evaluate the dynamic response of the charging system as a reactive power compensator, the reference of the instantaneous imaginary power (q_{ref}) is defined to be -10 kVAr from the instant t = 0 s and 10 kVAr after the instant t = 0.5 s.

The obtained results of the instantaneous real power (p) and the instantaneous imaginary power (q), and their respective references (p_{ref} and q_{ref}), are presented in Fig. 4 (a), while the obtained waveforms of the power grid voltage in phase a (v_a) and the grid current also in phase a (i_a), are presented in Fig. 4 (b). As expected, the instantaneous imaginary power follows its reference without sudden variations, demonstrating the fast dynamic response of the model predictive control.

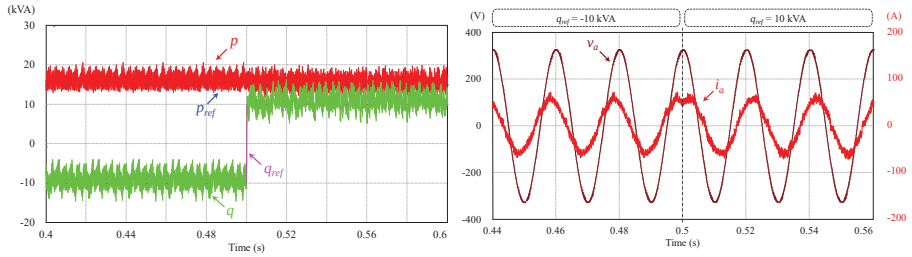

(a) (b)

Fig. 4. Simulation results of the fast EV battery charging process in transient-state: (a) Instantaneous p-q powers (p and q) and respective references (p_{ref} and q_{ref}); (b) Power grid voltage in phase a (v_a) and grid current also in phase a (i_a).

4 System Implementation

The developed laboratorial prototype can be divided in two main parts, the power converter and the digital control. The power converter is composed by a three-phase AC-DC power inverter and by a DC-DC. This converter is composed by four IGBTs legs, and it is used as EV motor drive or as fast EV battery charger. On the other hand, the digital control is composed by several circuits, predominantly by the DSC (TMS320F28335), the signal conditioning circuit (where is used an analog-to-digital converter to convert the signal from the sensors to the DSC), and the IGBTs gate drivers. The digital control is isolated from the power converters through hall-effect sensors and IGBTs gate drivers. The power converter and the digital control of the developed laboratorial prototype are presented in Fig. 5.

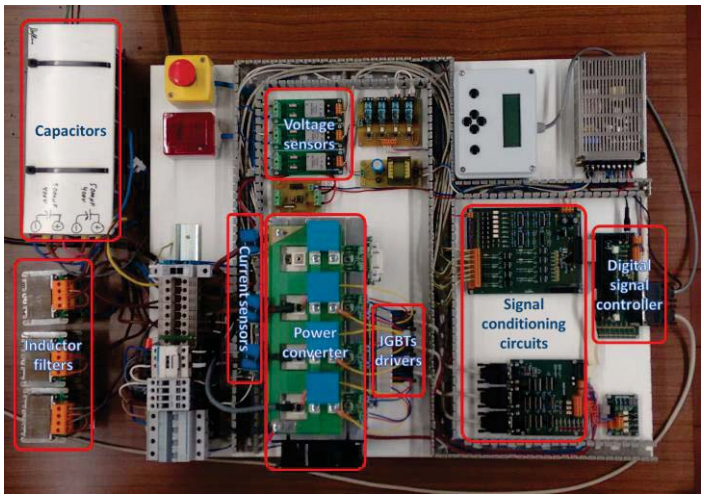

Fig. 5. Photograph of the developed laboratorial prototype.

5 Experimental Results

This section presents the main experimental results obtained with the developed laboratorial prototype. The experimental results were obtained with the developed laboratorial prototype connected to the power grid with a nominal voltage of about 75 V and a frequency of 50 Hz.

The first experimental results were obtained for an instantaneous real power (p_{ref}) of 1200 W and an instantaneous imaginary power (q_{ref}) of 0 VAr. Fig. 6 (a) shows the obtained results of the grid currents (i_a, i_b and i_c), as well as the voltage in DC-bus (v_{DC}). On the other hand, Fig. 6 (b) shows the experimental results of the power grid voltage (v_a) and the grid current (i_a). The harmonic spectrum and the RMS value of the grid current for the phase a (i_a) are presented in Fig. 7.

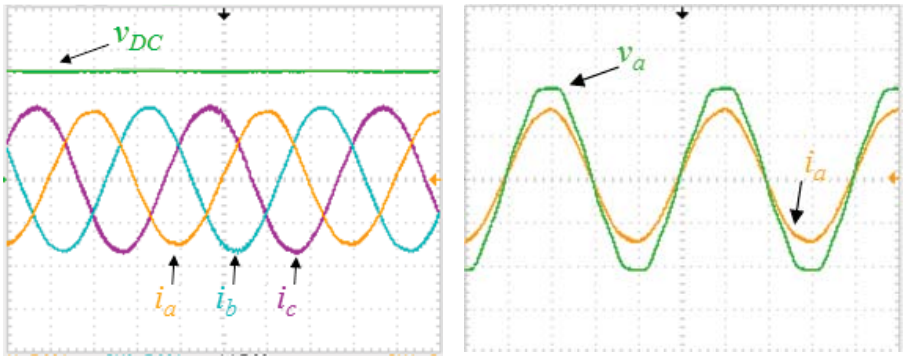

(a) (b)

Fig. 6. Experimental results of the fast EV battery charging process in steady-state: (a) Grid currents (i_a, i_b and i_c: 5 A/div), and DC-bus voltage (v_{DC}: 50 V/div); (b) Power grid voltage (v_a: 50 V/div) and grid current (i_a: 5 A/div).

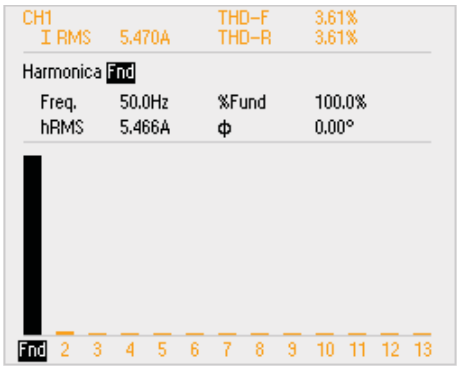

Fig. 7. Harmonic spectrum of the grid current for the phase a (i_a).

6 Conclusions

This paper presents an on-board fast battery charger for electric vehicle (EV) based on a model predictive control (MPC) algorithm.

The obtained simulation results allow validating the proposed control algorithms for the fast EV battery charger. The MPC permits to control the instantaneous real power (p) and the imaginary power (q) exchanged between the electrical grid and the EV battery charger, based on using a dynamical model of the system in order to predict its future behavior.

It was presented the operation of the EV battery charger with sinusoidal current and high power factor. These characteristics represent an important contribute, increasing the capabilities of the EVs and their potential role in order to improve the power quality of the electrical power grid.

The proposed integrated EV motor drive and EV battery charger applied to EVs contribute to optimize the space, weight and cost of the power electronics components inside the vehicle. The adopted topology allows fast EV battery charger operation, but needs extra inductor filters.

Acknowledgements

This work has been supported by COMPETE: POCI-01-0145-FEDER-007043 and FCT – Fundação para a Ciência e Tecnologia within the Project Scope: UID/CEC/00319/2013. Mr. Delfim Pedrosa was supported by the doctoral scholarship SFRH/BD/86628/2012 granted by the FCT agency.

References

1. Monteiro, V., Ferreira, J.C., Pinto, G., Pedrosa, D., Afonso, J.L.: iV2G Charging Platform. In: 13th International IEEE Conference on Intelligent Transportation Systems (ITSC), pp. 409–414. IEEE Press, Funchal (2010)

2. Haghbin, S., Khan, K., Zhao, S., Alaküla, M., Lundmark, S., Carlson, O.: An Integrated 20 kW Motor Drive and Isolated Battery Charger for Plug-In Vehicles. IEEE Transactions on Power Electronics, 28(8), 4013–4029 (2013)
3. Haghbin, S., Lundmark, S., Carlson, O., Alakula, M.: A Combined Motor/Drive/Battery Charger Based on a Split-Windings PMSM. In: IEEE Vehicle Power and Propulsion Conference (VPPC), pp. 1–6. IEEE Press, Chicago (2011)
4. Dusmez, S., Khaligh, A.: A Charge-Nonlinear-Carrier-Controlled Reduced-Part Single-Stage Integrated Power Electronics Interface for Automotive Applications. IEEE Transactions on Vehicular Technology, 63(3), 1091–1103 (2014)
5. Yilmaz, M., Krein, P.T.: Review of Charging Power Levels and Infrastructure for Plug-In Electric and Hybrid Vehicles. In: IEEE International Electric Vehicle Conference (IEVC), pp. 1–8. IEEE Press, Greenville (2012)
6. Yilmaz, M., Krein, P.T.: Review of Battery Charger Topologies, Charging Power Levels, and Infrastructure for Plug-In Electric and Hybrid Vehicles. IEEE Transactions on Power Electronics, 28(5), 2151–2169 (2013)
7. Sakr, N., Sadarnac, D., Gascher, A.: A Review of On-board Integrated Chargers for Electric Vehicles. In 16th European Conference on Power Electronics and Applications, pp. 1-10. IEEE Press, Lappeenranta (2014)
8. Pinto, J. G., Monteiro, V., Goncalves, H., Exposto, B., Pedrosa, D., Couto, C., Afonso, J.L.: Bidirectional Battery Charger with Grid-to-Vehicle, Vehicle-to-Grid and Vehicle-to-Home Technologies. In 39th Annual Conference of the IEEE industrial Electronics Society (IECON 2013), pp. 5934–5939. IEEE Press, Vienna (2013)
9. Haghbin, S., Khan, K., Lundmark, S., Alakula, M., Carlson, O., Leks, M., Wallmark, O.: Integrated Chargers for EV's and PHEV's: Examples and New Solutions. In XIX International Conference on Electrical Machines (ICEM), pp. 1–6. IEEE Press, Rome (2010)
10. Monteiro, V., Pedrosa, D., Exposto, B., Ferreira, J.C., Afonso, J.L.: Smart Charging System of the Electric Vehicle CEPIUM. In Annual Seminar on Automation, Industrial Electronics and Instrumentation (SAAEI'12), pp. 500–505 (2012)
11. Rodriguez, J., Kazmierkowski, M. P., Espinoza, J. R., Zanchetta, P., Abu-Rub, H., Young, H.A., Rojas, C.A.: State of the Art of Finite Control Set Model Predictive Control in Power Electronics. IEEE Transactions on Industrial Informatics, 9(2), 1003–1016 (2012)
12. Cortes, P., Rodriguez, J., Antoniewicz, P., Kazmierkowski, M.: Direct Power Control of an AFE Using Predictive Control. IEEE Transactions on Power Electronics, 23(5), 2516–2523 (2008)
13. Kouro, S., Cortes, P., Vargas, R., Ammann, U., Rodriguez, J.: Model Predictive Control - A Simple and Powerful Method to Control Power Converters. IEEE Transactions on Power Electronics, 56(6), 1826-1838 (2009)
14. Lim, J. S., Lee, Y.I1.: Model Predictive Control of Current and Voltage for Li-Ion Battery Charger using 3-Phase AC/DC Converter. In Proceedings of SICE Annual Conference 2010, pp. 215–218. IEEE Press, Taipei (2010)